

## FINAL REPORT

Research Grant No. NAG3-658  
for the period  
January 1986 - March 1995

FINAL  
IN-4LI-CR  
OCIT  
5961  
p.36

### Theoretical and Experimental Research in Space Photovoltaics

(NASA-CR-199698) THEORETICAL AND  
EXPERIMENTAL RESEARCH IN SPACE  
PHOTOVOLTAICS Final Report, Jan.  
1986 - Mar. 1995 (Cleveland State  
Univ.) 36 p

N96-14079

Unclass

Submitted to

G3/44 0075805

The NASA Lewis Research Center

by

The Cleveland State University

*Electrical Engineering Department, Space Photovoltaic Research Center*

November 6, 1995

Report prepared by the Principal Investigators:

Dr. Mircea Faur  
Dr. Maria Faur  
Senior Research Associates,  
Space Photovoltaic Research Center

## **1. Introduction**

Under a NASA-Lewis Research Center grant (No. NAG3-658), since 1986, the research group at CSU has conducted extensive theoretical and experimental research as outlined below (refs.1-59).

### **1.1 Theoretical Research on Space Solar Cells (refs. 1-14)**

#### **1.1.1 Theoretical Research on Indium Phosphide Solar Cells**

Under this project, FIESTA ROC, our new three dimensional finite element solar cell simulator computer code has been developed to accurately model the homojunction InP solar cell so as to provide a better understanding of the loss mechanisms and the precise locations of loss. This could aid in providing guidance to the experimental researchers on how to further optimize the solar cell design and improve its efficiency. Also, under this project, the homojunction InP solar has been simulated using our closed-form solution analytical computer model which has been used quite extensively up until now.

#### **1.1.2 Modelling of Other Solar Cells for Space Applications**

It was our intent to use FIESTA ROC extensively to model a variety of nonconcentrating and concentrating solar cells of several different semiconductor materials and device geometries for several different space applications.

One of the primary applications of FIESTA ROC, one for which it was developed, is to simulate the Point Contact Solar Cell (PCSC) at one sun and at high sunlight concentrations. Initially, some time was needed to incorporate databases of the material parameters of several semiconductors such as Si, GaAs, a-Si, etc. into FIESTA ROC. Once that is done, we intended to simulate the PCSC structure for various materials including Si, InP, GaAs and some other semiconductors, at one sun and at high sunlight concentrations for each material.

There is now growing interest in exploring the possibility of using thin film non-crystalline material, (e.g. CuInSe<sub>2</sub> polycrystalline thin film, amorphous Si, etc.) solar cells in space. Such cells, if they can be made to have beginning-of-life (BOL) 1 AMO, 25°C efficiency exceeding about 15%, have several advantages over the cells made from crystalline materials:

- 1) The thin film solar cells are comparatively very light weight and can be deposited on large plastic sheets or rolls. Such very light weight,

large area rolls of solar cells are easy to stow during launch and recovery of the space satellite and also easy to deploy after launch of the satellite in space.

2) The thin film solar cells are comparatively much less expensive on the basis of dollars/peak watt.

3) In laboratory radiation damage experiments, both the  $\alpha$ -Si and CuInSe<sub>2</sub> solar cells have shown a very high degree of radiation tolerance to 1MeV electrons and protons of various energies in comparison to crystalline semiconductor solar cells. Thus, if these noncrystalline material solar cells have the same high radiation tolerance in space as they do in the laboratory, a space satellite powered by these solar cells would have a much longer useful life in a high radiation environment such as the geosynchronous earth orbit (GEO).

Because of the above advantages, the noncrystalline material solar cells are of interest in space. It was our intent, under this project, to attempt to see if FIESTA ROC could be adapted to simulate the amorphous silicon and the CuInSe<sub>2</sub> polycrystalline solar cells.

Yet one more type of solar cell we would have liked to attempt to model using FIESTA ROC is the so-called JNLD solar cell which, in a recent publication in Applied Physics Letters (Vol. 60, No. 18, May 4, 1992, pp. 2240-2242) is claimed to have yielded an efficiency of 35% under nonconcentrated AM1.5 insolation. The JNLD cell is a crystalline silicon solar cell with a very thin layer of defects imbedded in the emitter very close to the junction space charge region. Ostensibly, the defects introduce midgap energy levels which allow electron hole pair production by two or more sub-bandgap photons acting in sequence in a multistep process. This allows the use of the sub-bandgap energy portion of the solar spectrum to generate electron-hole pairs, thereby significantly increasing the short-circuit current and the efficiency.

In terms of actual solar cell modeling done with FIESTA ROC, we succeeded in simulating the Si and InP conventional and PCSC cell geometries in the dark and at low light levels but ran into computer instability problems at 1 AMO and higher sunlight levels. Before we could fix the computer instability problem, we had to terminate any further work on FIESTA ROC due to the lack of resources. If, however, financial resources become available in the near future, then this work can be resumed and FIESTA ROC would be an excellent tool for accurately modeling most any kind of solar cell.

## **1.2 Fabrication and Performance Measurements of Shallow Homojunction InP Solar Cells for Space Applications (refs. 15-59)**

a) On unoptimized diffused  $n^+p$  (Cd,S)InP solar cells we have obtained a total area, AMO, 25°C efficiency of 14.35% which, while being comparatively low, is the highest reported value for cells fabricated on Cd-doped InP substrates. Based on our experimental studies we anticipate that by reducing the external losses due to poor contacts, by using optimized antireflection (AR) coatings and by passivating the surface, AMO, 25°C efficiencies greater than 18% are obtainable in our laboratory as compared to a peak efficiency of 16.6% reported by NTT Laboratories, Japan, for the same method of fabrication.

b) Using a surface science approach, high quality  $p^+n$  InP structures have been fabricated in our laboratory by thermal diffusion of Cd into n-InP substrates using thin phosphorus-rich anodic and chemical oxide cap layers. These structures have extremely low surface dislocation density of about 200-400  $\text{cm}^{-2}$ .

Based on our preliminary results on  $p^+n$  (cd,S)InP solar cells fabricated on these structures, we estimate total area, AMO, 25°C efficiencies of up to 21% to be achievable, providing that good quality contacts and AR coatings are used. So far, on these cells we have recorded a world record high open circuit voltage ( $V_{OC}$ ) of 890 mV (confirmed by NASA LeRC), which is higher than the  $V_{OC}$  of any previously reported  $V_{OC}$  of an InP solar cell made by any method of junction fabrication. However, due to poor contacts and AR coatings, our maximum AMO, 25 °C efficiency is only 13.2%, as compared to a maximum confirmed efficiency of 19.1% ( $V_{OC} = 876$  mV) on MOCVD-grown InP based solar cells fabricated by SPIRE Corporation.

## **1.3. Improved processing steps and InP material characterization with applications to fabrication of high efficiency radiation resistant InP solar cells and other opto-electronic InP devices.**

The interest in fabricating InP based devices was prompted after 1986 when the above-mentioned superior inherent qualities of InP as compared to other semiconductors such as Si and GaAs were first proved. Hence, very little information was available on changes in the physical and chemical properties of InP material under various processing steps. Therefore, to fabricate high quality InP devices an extensive experimental effort on the influence of most of the processing steps on the device characteristics was

necessary.

By adopting a surface science approach using surface analysis techniques such as x-ray photoelectron spectroscopy (XPS), Auger Electron Spectroscopy (AES), Scanning Electron Microscopy (SEM), Nomarski Microscopy, Energy Dispersive X-Ray Spectroscopy (EDAX), Secondary Ion Mass Spectrometry (SIMS), electrochemical C-V (EC-V) profiling, Photoluminescence Intensity (PLI), etc., in connection with solar cell performance parameters characterization, a systematic experimental program was undertaken in our laboratory in collaboration with NASA LeRC to determine the optimal processing parameters for improving the InP solar cell performance.

Although some of these studies have applications only to solar cell fabrication, most of them such as (a) various surface preparation techniques; (b) surface passivation; (c) junction formation; (d) surface dislocation density determination; (e) thinning down the emitter so as to obtain smooth, low dislocation density surfaces with good electrical characteristics; and (f) EC-V depth profiling, can be used for material characterization and/or as processing steps for other InP devices as well.

## **2. InP solar cells fabricated by thermal diffusion.**

### **2.1 Advantages:**

- ◆ lower processing costs due to the possibility of large-scale batch processing of large-area cells;
- ◆ high reproducibility of the diffusion process;
- ◆ more radiation resistant<sup>(\*)</sup> as compared to other InP cell structures (e.g. MOCVD-grown InP cells);
- ◆ radiation induced defect annealing under cell operating conditions<sup>(\*\*)</sup>, which is not observed in other InP-based cells or in Si or GaAs-based solar cells.

(\*) The high radiation tolerance of these cells, combined with their unique annealing behaviour under operating conditions, may eliminate the need for shunt circuits used in conventional satellites to dump excess power early in their missions.

(\*\*) Although InP has about twice the density of Si, the ability of diffused InP cells to anneal under operating conditions allows the thickness of the protective cover glass to be reduced, compensating for the difference in substrate weight.

## **2.2. $n^+p$ or $p^+n$ InP diffused cell structures?**

Until recently, the only InP solar cells fabricated by closed-ampoule thermal diffusion were those developed by NTT, Japan in the  $n^+p(S,Zn)$  configuration [GR1]. These cells proved to have high radiation tolerance, and independent studies [GR 2,3] have shown much higher annealing rates after irradiation, under the cell operating conditions, than high efficiency InP cells fabricated by MOCVD.

The drawback of the fabrication technique developed by NTT is that a large number of defects are present in the emitter layer after diffusion, which makes the solar cell efficiency lower than that of solar cells fabricated by epitaxy, due to a lower open circuit voltage  $V_{OC}$ . For example, for the best cell with AM0, 25°C efficiency of 16.6%., measured at NASA LeRC, the  $V_{OC}$  was 828 mV as compared to 876 mV for the higher AM0 efficiency (19.1%) MOCVD-grown cell [GR4].

## **2.3. Experiment-Based Predicted High Efficiency Solar Cells Fabricated by Closed-Ampoule Thermal Diffusion.**

Thermally diffused  $n^+p$  and  $p^+p$  InP solar cell structures [refs.15-59], were fabricated by us at CSU, by improving the technology developed by NTT, Japan, in the case of  $n^+p$  structures and by developing a new cell structure in the case of  $p^+n$  configuration.

For our cells, the ranking for experimental-based projected maximum cell efficiency, in decreasing order, was found to be: (1)  $p^+n$  (Cd,S); (2)  $n^+p$  (S,Cd); (3)  $p^+n$  (S,Zn); and (4)  $n^+p$  (Zn,S). Except for the  $p^+n$  (Cd,S) cells, the principal limiting factor for the other cell structures is  $V_{OC}$ . The large structural and electric-type defect density found in structures (2) to (4) as compared to the  $p^+n$  (Cd,S) structures, explains  $V_{OC}$  and  $\eta$  limitations of the last three structures also explains why, although a large effort was made by NTT to improve  $V_{OC}$  and efficiencies of diffused  $n^+p$  (S,Zn) cells, the reported maximum AM0 efficiency for these cells was of only 16.6% as compared to 19.1% reported for  $n^+p$  (Si,Zn) InP solar cells fabricated by MOCVD.

### **2.3.1 $n^+p$ InP Diffused Junction Solar Cells**

Based on our investigation the maximum achievable AM0, 25

AMOC efficiency of  $n^+p(S,Zn)$  InP diffused solar cells, developed by NTT, Japan is 18.2%, and 18.8% for  $n^+p(Cd,S)$  InP diffused solar cells, developed in our laboratory. The relatively low efficiencies of these cells as compared to all epitaxial-grown (MOCVD)  $n^+p$  InP solar cells, developed by Spire Corp., are due to a lower open circuit voltage ( $V_{OC}$ ), e.g. 828 mV for  $n^+p(S,Zn)$  and 840 mV for  $n^+p(S,Cd)$  as compared to 876 mV for epitaxially-grown  $n^+p(Si,Zn)$ InP cells. (see Table 1).

### 2.3.2. $p^+n(Cd,S)$ InP Diffused Junction Solar Cells.

At the 11th SPRAT Conference, we predicted that for homojunction InP solar cells made by thermal diffusion the  $p^+n$  configuration has a higher efficiency than the  $n^+p$  configuration due especially to an increased  $V_{OC}$ . The prediction was based on AMO, 25°C  $V_{OC}$  values of 860 mV we measured for  $p^+n(Cd,S)$  InP solar cells as compared to experiment-based projected  $V_{OC}$  of only 840 mV for our  $n^+p(S,Cd)$  InP solar cells. In 1993 on bare  $p^+n(Cd,S)$  InP diffused cells we recorded AMO, 25°C  $V_{OC}$  values of 880.3 mV which, as seen in Table 1, are higher than those reported for thermally diffused and epitaxially grown  $p^+n$  InP cells with optimized AR coating and higher even than the highest reported for all MOCVD-grown  $n^+pp^+$  InP solar cells -- 876 mV -- which corresponds to the maximum reported AMO efficiency of 19.1% for an InP solar cell. Recently, by using improved  $p^+n(Cd,S)$  InP structures, the AMO, 25°C recorded  $V_{OC}$  values were from 881 to 887.6 mV (Table 2), using an unoptimized chemical oxide layer as an AR coating. The highest AMO efficiency, on a bare cell was 13.2%. The relatively low efficiency is mainly due to a very high series resistance ( $R_S$ ) and correspondingly low fill factor (FF) as well as to the fact that no AR coating except for the thin (20 to 40 nm) chemical oxide passivating layer was used. As an example, by using an unoptimized single layer SiO ( $\sim 70$  nm) AR coating the short circuit current density,  $J_{SC}$ , have increased from 27.59 mA/cm<sup>2</sup> (see Table 2) to 30.95 mA/cm<sup>2</sup>, which is in good agreement to overall reflexivity decrease from about 29% using the thin P-rich chemical oxide to about 21%, using the SiO single layer AR coating. Since the reflexivity of a well designed ZnS/MgF<sub>2</sub> double layer AR coating has an overall reflexivity of only 2 to 5%, by using it, the expected maximum  $J_{SC}$  of this cell should be from 37.2 to 38.4 mA/cm<sup>2</sup>. From the  $I_{SC}$ - $V_{OC}$  characteristics the additional increase in Voc of 8 to 10 mV is expected, which will make the Voc of this cell from 895 to 897 mV. Assuming that the FF can be increased from 61.5% to only 80%, the expected AMO, 25°C efficiency is about 19.8%.

InP diffused cells we recorded AMO, 25°C  $V_{OC}$  values of 880.3 mV which, as seen in Table 1, are higher than those reported for thermally diffused and epitaxially grown  $p^+n$  InP cells with optimized AR coating and higher even than the highest reported for all MOCVD-grown  $n^+pp^+$  InP solar cells -- 876 mV -- which corresponds to the maximum reported AMO efficiency of 19.1% for an InP solar cell. Recently, by using improved  $p^+n(Cd,S)$  InP structures, the AMO, 25°C recorded  $V_{OC}$  values were from 881 to 887.6 mV (Table 2), using an unoptimized chemical oxide layer as an AR coating. The highest AMO efficiency, on a bare cell was 13.2%. The relatively low efficiency is mainly due to a very high series resistance ( $R_S$ ) and correspondingly low fill factor (FF) as well as to the fact that no AR coating except for the thin (20 to 40 nm) chemical oxide passivating layer was used. As an example, by using an unoptimized single layer SiO (~ 70 nm) AR coating the short circuit current density,  $J_{SC}$ , have increased from 27.59 mA/cm<sup>2</sup> (see Table 2) to 30.95 mA/cm<sup>2</sup>, which is in good agreement to overall reflexivity decrease from about 29% using the thin P-rich chemical oxide to about 21%, using the SiO single layer AR coating. Since the reflexivity of a well designed ZnS/MgF<sub>2</sub> double layer AR coating has an overall reflexivity of only 2 to 5%, by using it, the expected maximum  $J_{SC}$  of this cell should be from 37.2 to 38.4 mA/cm<sup>2</sup>. From the  $I_{SC}$ - $V_{OC}$  characteristics the additional increase in  $V_{OC}$  of 8 to 10 mV is expected, which will make the  $V_{OC}$  of this cell from 895 to 897 mV. Assuming that the FF can be increased from 61.5% to only 80%, the expected AMO, 25°C efficiency is about 19.8%.

Since, of all solar cell parameters,  $V_{OC}$  can be regarded as the best measure of how low is the defect density within a given structure from among the different cell structures, its value can give useful information about the quality of each cell structure. Recently [10], using a P-rich passivating layer grown by chemical oxidation, we have succeeded in fabricating diffused junction  $p^+n(Cd,S)$  InP solar cells with measured AMO, 25 °C  $V_{OC}$  of 890 mV for a 1 cm<sup>2</sup> cell, which to the best of our knowledge are higher than previously reported  $V_{OC}$  values for any InP homojunction solar cells. The achievement of such high  $V_{OC}$  value for a diffused junction cell with no AR coating, except for the residual oxide layer, which covers the surface after thinning the emitter, is remarkable if one takes into consideration that the InP:S LEC grown substrates used have had a rather large EPD of  $5-7 \times 10^4$  cm<sup>-2</sup>.

The low AMO, 25°C efficiency of  $p^+n(Cd,S)$  InP cell of only 13.2% can be explained by the very large thickness of the emitter (0.62  $\mu$ m), a large front grid coverage (13.15%) and the absence of an AR coating. The cell shows a surprisingly good blue response for an emitter as thick as 0.62  $\mu$ m, indicating a highly passivated surface and a large minority carrier diffusion length in the emitter. The cell had a high series resistance of about 3  $\Omega$ -cm<sup>2</sup>



due to high contact and sheet resistances, resulting in a low fill factor (FF) of 73.1% and low efficiency.

By using an optimized two-layer AR coating (e.g. P-rich chemical oxide/ $\text{Al}_2\text{O}_3/\text{MgF}_2$ , and reducing the grid shadowing to 6%, the projected  $J_{\text{SC}}$  value for a  $0.3\ \mu\text{m}$  thick emitter is  $38.2\ \text{mA}/\text{cm}^2$ , and  $V_{\text{OC}} > 895\ \text{mV}$ . Should it be possible to deposit ohmic front contacts ( $4\text{--}5\ \mu\text{m}$  thick) on thin emitters (i.e. up to  $1\ \mu\text{m}$  thick) without short-circuiting the junction, then the projected FF of these cells should be about 84% and the projected AM0,  $25^\circ\text{C}$  efficiency about 20.9%.

As seen in Table 3, by using our state-of-the-art  $p^+n$  structures with a surface concentration of  $4 \times 10^{18}\text{cm}^{-3}$ , we project the maximum achievable efficiency to be 21.3%. The relatively large increase in  $V_{\text{OC}}$ , from our presently projected value of 895 mV to 910 mV, is based not only on a  $V_{\text{OC}}$  increase with the expected increase in  $I_{\text{SC}}$  by using an optimized AR coating, but on our latest experimental data which show that further improvement in surface passivation is possible. Even higher  $V_{\text{OC}}$  values, approaching 930 mV, are possible by using better quality substrates (i.e. with EPD below  $10^4\ \text{cm}^{-2}$ ), optimizing base doping, and by further optimizing the diffusion process and the quality of the passivating layer.

#### 2.4. Radiation Resistance of Diffused Junction InP Solar Cells.

A preliminary investigation of  $p^+n$  (Cd,S),  $n^+p$  (S,Cd) and  $p^+n$  (Zn,S) thermally diffused InP structures and solar cells, prior to and after irradiation with  $10^{13}\text{cm}^{-2}$  3 MeV protons, indicates that the same ranking holds for these three structures with respect to radiation tolerance as mentioned above for maximum efficiency. The  $p^+$  emitters of  $p^+n$  (Cd,S) InP diffused structures show very low radiation-induced carrier removal rates as compared to either  $p^+n$  (Zn,S) or  $n^+p$  (S,Cd) InP diffused structures, and a remarkable annealing property at room temperature in the dark.

Preliminary results of radiation resistance studies of diffused  $p^+n$  (Cd,S) InP solar cells, indicate that the percent of remaining power (39%), after irradiation with  $10^{13}\ \text{cm}^{-2}$ , 3 MeV protons (Table 4) is higher than that of other InP cell structures, including the all-MOCVD fabricated  $n^+p$  (Si,Zn) and diffused  $n^+p$  (S,Zn) InP cells, for which irradiation data using 3 MeV protons are available. Furthermore, this cell shows a remarkable annealing property at room temperature (RT) in the dark. The AM0,  $25^\circ\text{C}$ , performance parameters of this cell prior to irradiation and after about 1 year at RT in the dark, are shown in Table 5. Subsequent light soaking of this cell for 1 hour under

AM1.5, 25 °C, raised its efficiency by about 2.5% , indicating good annealing properties under illumination.

Preliminary radiation resistance studies and annealing studies of these cells have been started at Spire Corp., after irradiation with high energy alpha particles. For one such cell, for which data are available, after irradiation at an equivalent 1MeV  $e^-$  fluence of  $1.06 \times 10^{17} e^-/\text{cm}^2$ , which corresponds to over 100 years in GEO, the remaining power output is 32% of the initial power (Table 6). As a result of a significant recovery of about 6%, after only 4 days at RT in the dark, and an expected higher recovery rate under the cell operating conditions (RT, under illumination), these cells are not expected to degrade significantly in high radiation environment orbits, even after such large fluences.

We attribute the high radiation resistance of diffused  $p^+n$  (Cd,S) InP cells to a relatively much lower irradiation induced carrier removal rate in the emitter as compared to the InP:S base. For a thick  $p^+$  emitter, most of the cell current is not expected to come from the base or space charge region. Since the Cd-diffused emitter degrades less than the low doped base, the superior radiation resistance of these cells, as compared to a  $n^+p$  configuration with a thin emitter (e.g. 40 nm), should be expected.

### **3. Chemical and Electrochemical Characterization and Processing of InP Diffused Structures and Solar Cells.**

In this work we have focused on the use of photoelectrochemical techniques for characterization of InP and related material structures. The work did focus on both the characterization and step-by-step optimization of  $n^+p$  and  $p^+n$  InP structures fabricated by thermal diffusion, with application to fabrication of high efficiency, radiation resistant InP solar cells by this method of junction formation. The emitter layer and the junction proximity of the base are characterized as functions of: (a) various surface preparation procedures; (b) diffusion cap; (c) diffusion source, and (d) diffusion conditions (diffusion temperature and time, amount of source material and added phosphorus, and temperature difference between the source and substrates). The EC characteristics of the emitter layer provides: (a) thicknesses of front oxide and damaged layers; (b) density of surface and deep dislocation and precipitates; (c) net majority carrier concentration depth profile, and (d) surface and deep trap level density. The EC characterization was done before and after irradiating the structures with high energy electrons and protons.

In order to maximize the solar cell performances, we also investigated different post-diffusion surface preparation procedures such as removal of the front damaged emitter layer and subsequent surface passivation to obtain smooth, low defect density surfaces with good electrical characteristics.

A step-by-step EC characterization of  $n^+p$  (S,Zn),  $n^+p$  (S,Cd),  $p^+n$  (Zn,S) and  $p^+n$  (Cd,S) InP structures, fabricated by thermal diffusion, as a function of processing parameters has helped us not only to improve the fabrication process of diffused structures but also to predict the  $J_{SC}$  and  $V_{OC}$  values of solar cells made from these structures. The main research areas we have undertaken in C and EC characterization of diffused structures and as solar cell fabrication steps include:

- EC Characterization of InP Diffused Structures:
  - EC-V Profiling
  - Structural Defects
  - Electrical Defects
- Solar Cells
  - Step-by-step EC-V Characterization of InP Diffused Structures
  - Chemical (C) and Electrochemical (EC) Fabrication Steps
    - C and EC Thinning
    - Diffusion Cap Layers
    - Surface Passivation
    - Electroplated Front Contacts
    - First Layer AR Coating
  - EC-V Prediction of Performance Parameters

For performing such an extensive experimental task EC techniques are much faster and could be more reliable as compared to solid-state techniques. They allow one to study not only the global picture of one of the characteristics of interest as is the case with most of the solid-state techniques but also the variation of these characteristics at different depths throughout the structures.

A significant improvement in the quality of  $n^+p$  and  $p^+n$  InP structures fabricated by closed-ampoule thermal diffusion was obtained after optimizing the diffusion processing using EC techniques for step-by-step characterization of these structures. The investigation was designed to establish: (i) a proper surface preparation procedure prior to diffusion for the substrates; (ii) the right

dopant for the substrates and the right diffusant; (iii) the nature and thickness of the diffusion cap layer; (iv) diffusion temperature and amounts of source materials for doping the substrates below the solubility limit of the doping species; (v) diffusion time for obtaining a desired junction depth; (vi) temperature difference between the substrates and source zones; (vii) thickness of the front dead layer, and (viii) the post-diffusion surface preparation procedure for the removal of the front damaged layer of the surface so as to obtain smooth passivated surfaces with good electrical characteristics.

As an example, a significant reduction of structural defect densities of  $n^+p$  and  $p^+n$  InP structures was obtained after optimizing the diffusion process, as can be seen in Tables 7 and 8. For  $n^+p$  structures, the lowest etch pit density (EPD) of  $6 \times 10^5 \text{ cm}^{-2}$  was achieved after S diffusion into InP:Cd ( $N_A \approx 1.2 \times 10^{16} \text{ cm}^{-3}$ ) substrates using a thin  $\text{In}(\text{PO}_3)_3$ -rich anodic oxide diffusion cap layer at a diffusion temperature of  $660^\circ\text{C}$ , while the lowest EPD after S diffusion into InP:Zn ( $N_A \approx 2 \times 10^{16} \text{ cm}^{-3}$ ) under similar diffusion conditions was  $8 \times 10^6 \text{ cm}^{-2}$ . For  $p^+n$  structures, surface EPD values as low as  $2 \times 10^2 \text{ cm}^{-2}$  were achieved in the case of Cd diffusion into InP:S ( $N_D = 3.5 \times 10^{16} \text{ cm}^{-3}$ ) substrates at a diffusion temperature of  $560^\circ\text{C}$  using a thin  $\text{In}(\text{PO}_3)_3$ -rich chemical oxide diffusion cap layer, while the lowest EPD in the case of Zn diffusion was  $3 \times 10^5 \text{ cm}^{-2}$ . The differences are explained by the large number of  $\text{In}_2\text{S}_3$ ,  $\text{InS}$  and  $\text{Zn}_3\text{P}_2$  surface and deep precipitates detected in the case of  $n^+p$  (S,Zn) and  $p^+n$  (Zn,S) InP structures.

From the EC characteristics for our diffused structures, we found the ranking in decreasing order of projected maximum efficiency to be: (1)  $p^+n$  (Cd,S), (2)  $n^+p$  (S,Cd), (3)  $p^+n$  (Zn,S), (4)  $n^+p$  (S,Zn). The AMO,  $25^\circ\text{C}$  efficiency of solar cells fabricated on these structures have confirmed that the maximum efficiency could be obtained in the case of  $p^+n$  (Cd,S) solar cells while the worst performances were recorded in the case of  $n^+p$  (S,Zn) cells. A preliminary EC investigation of  $p^+n$  (Cd,S),  $n^+p$  (S,Cd) and  $p^+n$  (Zn,S) structures both prior to and after irradiation with  $10^{13} \text{ cm}^{-2}$  of 3 MeV protons, which includes studies of electrical and structural defect densities and net majority carrier concentration variations in the emitter and the immediate junction proximity of the base, seems to indicate that the same ranking as above holds for radiation tolerance.

A new etchant namely,  $(\text{o-H}_3\text{PO}_4)_u:(\text{HNO}_3)_v:(\text{H}_2\text{O}_2)_t:\text{H}_2\text{O}_{1-(u+v+t)}$ , which we have called the "PNP" etchant, has been developed for thinning the  $p^+$  emitter layer of  $p^+n$  InP structures, so as to obtain stable, smooth surfaces with good opto-electronic characteristics for application in  $p^+n$  InP solar cell fabrication. Varying  $u$ ,  $v$  and  $t$ , reproducible etch rates of 5 to 110

nm/min have been measured. After thinning the 0.6 to 2.5  $\mu\text{m}$  thick  $\text{p}^+$  layer down to 60-250 nm of  $\text{p}^+\text{n}$  InP solar cells made by thermal diffusion of Cd into InP:S substrates, specular surfaces have been obtained at up to 80 nm/min etch rate.

Thinning of  $\text{p}^+$  InP using this etchant is superior to that using previously reported etchants based on  $\text{HBr}:\text{COOH}$ ,  $\text{HCl}$  and  $\text{HNO}_3$  as well as by anodic oxidation-removal cycles because of the following properties: a) thinning can be accomplished on an already metallized  $\text{p}^+$  InP emitter layer, b) low dissolution rate makes thinning process easily controlled, c) this etchant is non-defect revealing, d) it yields stable surfaces with good passivating properties, and e) it grows an oxide layer with good optoelectronic characteristics for possible use as a first layer antireflection (AR) coating.

A new electrolyte (FAP) was developed for EC-V profiling of InP diffused structures. This electrolyte was developed since none of the previously recommended electrolytes (see Table 9) work well with InP. This electrolyte is recommended by BIORAD, the makers of Polaron EC-V profilers for accurate EC-V profiling of InP. It, however, does not work well with other InP and GaAs based compounds.

A new electrolyte (UNIEL) we developed for EC-V profiling of InP and GaAs based structures [7]. The composition of the UNIEL electrolyte is: A-B-C (1 : 4 : 1), where:

Solution A: 48% HF : 99%  $\text{CH}_3\text{COOH}$  : 85% o- $\text{H}_3\text{PO}_4$  :  $\text{H}_2\text{O}$   
(5 : 1 : 2 : 100) ;

Solution B: 0.1 M N-n-Butylpyridinium Chloride ( $\text{C}_9\text{H}_{14}\text{ClN}$ ), and  
Solution C: 1 M  $\text{NH}_3\text{F}_2$ .

Solution A works very well with InP layers. However, although it works with GaAs layers, the accuracy of EC-V profiles in this case is rather poor due to a high chemical etch rate of GaAs of up to 0.5 m/hour. Solution B works well with GaAs layers. However, due to insoluble oxide formation on the etched surface, it cannot be used for InP layers. A combination of solution A: solution B (1:4) can be used for EC-V profiling of InP, GaAs and InGaAs layers. However, due to an incomplete dissolution of anodic oxides in the case of InGaAsP layers, we have found a combination of solutions A:B:C (1:4:1), which we call the UNIEL electrolyte, to be a very good choice for profiling of InP and GaAs based multi-layer structures.

The UNIEL electrolyte has been tested with very good results for EC-V profiling of a large number of structures made of n- and p-type InP, GaAs, InGaAs and InGaAsP layers. Generally, using the UNIEL electrolyte, accurate

EC-V profiles are obtained when the anodic dissolution current density is from 0.5 to 1.5 mA/cm<sup>2</sup>. The anodic dissolution rate under these conditions is from 0.8 to 1.5 m/hour.mA/cm<sup>2</sup>, that is much higher than the chemical etch rate, which for all tested materials is less than 0.015 m/hour. Except for the lightly doped InGaAsP, the craters have smooth bottoms with straight walls, and the calculated crater depths agree within 5% with Dektak measured values.

### **Alternate Uses of the FAP (for InP) and UNIEL Electrolyte for Characterization of InP and GaAs Based Structures**

Due to their intrinsic characteristics the FAP and UNIEL electrolytes can be used for EC determination of:

- \* Flat-band (Built-in) Potential
- \* Existence and Thickness of Native Oxides
- \* Bandgap
- \* Band Offsets
- \* Diffusion Length and Lifetime of Minority Carriers
- \* Surface Recombination Velocity (SRV)

As a process control tool, EC techniques are faster and of reduced complexity compared to solid-state techniques. In addition, the use of EC techniques allows in-situ recording of a large number of semiconductor characteristics at different depths throughout the structure and, in a multilayer structure, within each layer and at the interfaces.

It is our opinion that EC techniques are or could become more accurate than any known solid-state techniques for performing majority and possibly minority doping concentration depth profilings, as well as for the mapping of structural and electrical type defect densities as functions of depth.

Using improved EC characterization techniques for step-by-step optimization of n<sup>+</sup>p and p<sup>+</sup>n InP diffused structures has made it possible to fabricate high performance homojunction InP structures.

## 4. Progress in $p^+n$ InP Diffused Solar Cells

Our efforts over the last two years or so were concentrated on designing: 1) thin  $p^+$ -InP emitters, 2) front contacts, 3) passivating layer and 4) AR coating, so as to minimize the large external losses present in our cells.

### 4.1. Thin Emitters.

For cells such as that shown in Table 2, thick emitters have been used. This adds a troublesome fabrication step, which affects the reproducibility of cell performances. Furthermore, using thick emitters thinning from over  $4\text{ }\mu\text{m}$  to below  $0.5\text{ }\mu\text{m}$  has the drawback of reducing the surface hole concentration in the thinned emitter, thereby increasing the series resistance ( $R_s$ ) and lowering the fill factor (FF). Since the optimal emitter thickness is estimated at about  $0.25$  to  $0.3\text{ }\mu\text{m}$ , we were able to fabricate thin emitters ( $0.5$  to  $0.75\text{ }\mu\text{m}$ ) while maintaining the high surface acceptor concentration.

### 4.2 Electroplated Front Contacts.

For thin emitters ( $0.5$  to  $0.75\text{ }\mu\text{m}$ ) we first tried thin ( $0.1\text{ }\mu\text{m}$ ) Au-Zn evaporated contacts, with an intent to then deposit thicker electroplated contacts after sintering. However, after sintering the contacts at  $430\text{ }^\circ\text{C}$ , for 2 minutes, the contacts penetrated at depths greater than the emitter thickness, short-circuiting it. For lower sintering temperatures the contacts lifted during subsequent chemical treatments in PNP etch we are using both for surface passivation and thinning the emitter. For these samples, after removing the evaporated contacts, Au-Zn and Au-Cd ( $\sim 0.5\%$  Zn or Cd) front contacts were fabricated using conventional UV lithography and electroplating. The positive photoresist ( $\sim 5\text{ }\mu\text{m}$  thick) was deposited on clean and chemically oxidized emitter surfaces. In both cases about  $0.5\text{ }\mu\text{m}$  Au-Zn or Au-Cd were first electrodeposited by pulse plating at pulse current density of  $0.5$  to  $2\text{ mA/cm}^2$ , then  $5$  to  $18\text{ }\mu\text{m}$  Au was deposited at a constant current density of  $0.2$  to  $0.3\text{ mA/cm}^2$ . When using clean surfaces the width of the contact grid fingers became up to 3 times the designed values, while their width have not increased significantly when a  $20$  to  $50\text{ nm}$  chemical oxide was used. Electroplated Au-Zn or Au-Cd front contacts we found are well suited for deposition on thin emitters since they do not require sintering. For example, using  $\sim 8\text{ }\mu\text{m}$  thick electroplated Au-Zn contacts, grown on a  $0.6\text{ }\mu\text{m}$  thick emitter, using an oxidized surface, we recorded  $R_s$  values as low as  $1.14$

$\Omega\text{-cm}^2$ , and FF values of over 82%, after thinning the emitter to about  $0.35\text{ }\mu\text{m}$ . Since for p/n configuration the sheet resistance is a major contributor to  $R_s$ , we estimate that by using an optimized front grid mask with  $250\text{ }\mu\text{m}$  between the lines instead of presently used  $620\text{ }\mu\text{m}$ ,  $R_s$  values of less than  $0.5\text{ }\Omega\text{-cm}^2$  and FF greater than 84% can be achieved after thinning the  $p^+$  emitter to  $0.25\text{-}0.3\text{ }\mu\text{m}$ .

### 4.3 Surface Passivation

One of the key factors limiting the performance of InP solar cells is their high surface recombination velocity (SRV), which is estimated, even for epitaxially grown cells to be as high as  $10^7\text{ cm/s}$ . Although not near to such an extent as the  $n^+p$  InP structures,  $p^+n$  InP structures fabricated by thermal diffusion have their surface stoichiometry destroyed. Therefore, it is important in the fabrication of high-performance InP solar cells in general and diffused InP cells in particular, to remove in a controlled manner the high defect density surface layer of the emitter and to passivate the surface. Calculations have shown that SRVs higher than  $5 \times 10^5\text{ cm/s}$  drastically reduce the efficiency of InP solar cells by lowering their blue response. Simple chemical treatments of InP surfaces using  $\text{HNO}_3$  and HF based etchants were found to decrease the SRV to below  $5 \times 10^5\text{ cm/s}$ , e.g.  $1.7 \times 10^5$  for  $n^+ \text{-InP}$  and  $4.7 \times 10^5\text{ cm/s}$  for  $p^+ \text{-InP}$ , after rinsing the substrates in a  $\text{HNO}_3$  (15%) solution.

Using the PNP etch, based on  $\text{HNO}_3$ ,  $o\text{-H}_3\text{PO}_4$ , and  $\text{H}_2\text{O}_2$ , we developed for thinning after contacting the  $p^+ \text{-InP}$  emitter, from low frequency EG-V measurements, we recorded a surface state density minimum ( $N_{ss}$ ) at the Cd-diffused  $p^+ \text{-InP}$ /passivating layer interface as low as  $2 \times 10^{10}\text{ cm}^{-2}\text{ eV}^{-1}$ . About  $40\text{ nm}$  was removed from the surface of a the  $p^+n$  InP structure diffused at  $660\text{ }^\circ\text{C}$  (surface acceptor concentration:  $\sim 4 \times 10^{18}\text{ cm}^{-3}$ ; junction depth:  $\sim 3.5\text{ }\mu\text{m}$ ). Such a low  $N_{ss}$  value is in good qualitative agreement with the high measured  $V_{oc}$  and blue response values of solar cells fabricated on these structures.

### 4.4. AR Coating

It is well known that the behavior of III-V compound based solar cells is largely controlled by their surface, since the majority of light generated carriers (63% for GaAs and 79% for InP) are created within  $0.2\text{ }\mu\text{m}$  of the illuminated surface of the cell. Consequently, the always observed high surface recombination velocity (SRV) on these cells is a serious limiting factor for their high efficiency performance, especially for those with the p-n junction made by either thermal diffusion or ion implantation. A good surface passivation



layer, ideally, a grown oxide as opposed to a deposited one, will cause a significant reduction in the SRV without adding interface problems, thus improving the performance of III-V compound based solar cells. Another significant benefit to the overall performance of the solar cells can be achieved by a substantial reduction of their large surface optical reflection by the use of a well designed antireflection (AR) coating.

We demonstrated the effectiveness of using a chemically grown, thermally and chemically stable oxide, not only for surface passivation but also as an integral part of a 3-layer AR coating for thermally diffused  $p^+n$  InP solar cells. A phosphorus-rich interfacial oxide,  $\text{In}(\text{PO}_3)_3$ , is grown at the surface of the  $p^+$  emitter using an etchant based on  $\text{HNO}_3$ ,  $\text{o-H}_3\text{PO}_4$  and  $\text{H}_2\text{O}_2$ . This oxide has the unique properties of passivating the surface as well as serving as a fairly efficient antireflective layer yielding a measured record high AM0, 25°C, open-circuit voltage of 890.3 mV on a thermally diffused InP(Cd,S) solar cell. Unlike conventional single layer AR coatings such as ZnS,  $\text{Sb}_2\text{O}_3$ , SiO or double layer AR coatings such as ZnS/MgF<sub>2</sub> deposited by e-beam or resistive evaporation, this oxide preserves the stoichiometry of the InP surface. We show that it is possible to design a three-layer AR coating for a thermally diffused InP solar cell using the  $\text{In}(\text{PO}_3)_3$  grown oxide as the first layer and  $\text{Al}_2\text{O}_3$ , MgF<sub>2</sub> or ZnS, MgF<sub>2</sub> as the second and third layers respectively, so as to yield an overall theoretical reflectance of less than 2% (see Figure 1).

Since chemical oxides are readily grown on III-V semiconductor materials, the technique of using the grown oxide layer to both passivate the surface as well as serve as the first of a multilayer AR coating, should work well for essentially all III-V compound-based solar cells.

The residual oxide grown on  $p^+$ -InP using the PNP etch is composed of a thick In-rich outer layer and a P-rich layer at the interface with the emitter. From XPS investigation, the interfacial oxide is rich in  $\text{In}(\text{PO}_3)_3$ . Since this oxide, as seen above, passivates the surface quite well, and it has a bandgap of  $6.8 \pm 0.2$  eV [17] we proposed that it be used as a first layer AR coating. The transparency of this oxide over the measured 1.8 to 5.2 eV range and its low blue reflectivity, as compared to SiO,  $\text{Sb}_2\text{O}_3$ , and optimized ZnS/MgF<sub>2</sub> double layer AR coating, seem to make this oxide a very attractive candidate, indeed, for use as a first layer AR coating. In addition, when we deposited on our bare  $p^+n$  InP cells either SiO or  $\text{Sb}_2\text{O}_3$  or a double layer of ZnS/MgF<sub>2</sub>, the  $V_{oc}$  dropped by as much as 50 mV, indicating a large increase in SRV.

As shown in Fig.2, the two layered oxide (~ 130 nm) reduces the reflectance of an  $p^+n$  InP solar cell from an average of 40% to slightly less than 20%. In this particular case, after removing the In-rich outer-oxide layer, the reflectance of the remaining thin  $\text{In}(\text{PO}_3)_3$  oxide is about 26%. Although the overall reflectance of the double-layered chemical oxide in Fig.3 is lower

than that of SiO<sub>2</sub>, it is still too high for use as a single layer AR coating. Furthermore, the outer In-rich oxide is unstable and quite conductive, which caused for our cells a noticeable drop in  $R_{sh}$ , and  $V_{oc}$ . Therefore, we removed it, and in our best design we add Al<sub>2</sub>O<sub>3</sub> and MgF<sub>2</sub> as second and third layers of the three-layer coating. For the example in Fig.2, a three-layer AR coating composed of In(PO<sub>3</sub>)<sub>3</sub> (45 nm) / Al<sub>2</sub>O<sub>3</sub> (62 nm) / MgF<sub>2</sub> (41 nm), reduces the overall reflectivity (no grid fingers) to less than 2%.

From correlations between measured cell parameters, reflectivity, spectral response, dark saturation current densities and  $J_{sc}$ - $V_{oc}$  plots, the projected maximum practically achievable AM0, 25 °C performance parameters of p<sup>+</sup>n (Cd,S) InP solar cells, using our state-of-the-art newly developed thin emitters, and optimal front grid (6% coverage), and the newly designed three layer AR coating, are:  $V_{oc}$ =910 mV,  $J_{sc}$ =38.6 mA/cm<sup>2</sup>, FF=84%, and  $\eta$ =21.3%. These performances are predicted for an emitter thickness of 0.3  $\mu$ m, a surface acceptor concentration of  $3.5 \times 10^{18}$  cm<sup>-3</sup>, base electron concentration of  $7.5 \times 10^{16}$  cm<sup>-3</sup>, front SRV of  $10^5$  cm/s, and using LEC grown InP:S substrates with EPD= $5 \times 10^4$  cm<sup>-2</sup>. Higher efficiency is possible by using better quality substrates, further improving the diffused structures and the cell fabrication sequences.

## REFERENCES (R)

1. C. Goradia, W. Thesling and I. Weinberg, "Theoretical Modeling, Near-Optimum Design and Predicated Performance on  $n^+pp^+$  and  $p^+nn^+$  Indium Phosphide Homojunction Solar Cells", Proceedings of the 22nd IEEE Photovoltaics Specialists Conference, Las Vegas, Nevada, October 7-11, 1991, pp. 209-215.
2. C. Goradia, W. Thesling, and I. Weinberg, "A Theoretical Comparison of the Near-Optimum Design and Predicated Performance of  $n/p$  and  $p/n$  Indium Phosphide Homojunction Solar Cells", Proceedings of the Eleventh Space Photovoltaic Research and Technology Conference, NASA LeRC, Cleveland, Ohio, May 7-9, 1991, pp. 30-1 to 30-10.
3. R. Lowe, C. Goradia, M. Goradia and Donald L. Chubb, "Study of a Cesium Plasma as a Selective Emitter for Thermophotovoltaic Applications", J. Appl. Phys. 68 (10), pp. 5033-5035, 15 November, 1990.
4. C. Goradia, W. Thesling and I. Weinberg, "Key Factors Limiting the Open Circuit Voltage of  $n^+pp^+$  Indium Phosphide Solar Cells", Conference Record of the 21st IEEE Photovoltaic Specialists Conf., May 21-25, 1990, Orlando, Florida, pp. 386-393.
5. Chandra Goradia, William Thesling, and Irving Weinberg, "Key Factors Limiting the Open Circuit Voltage of Indium Phosphide Solar Cells", Proc. 10th Space Photovoltaic Research and Technology Conf., NASA LeRC, Cleveland, Ohio Nov. 7-9, 1989, pp. 298-310.
6. C. Goradia, J.V. Geier and I. Weinberg, "Theory of the InP Shallow Homojunction Solar Cell", SOLAR CELLS, Vol. 25, pp. 235-253, 1988.
7. R.O. Clark, C. Goradia, D.J. Brinker, "Dependence of Lifetime on Design Parameters of an  $nipi$  Doping Superlattice: Results of Self-consistent Calculations", Superlattices and Microstructures, Vol. 4, No. 2, 1988, pp. 187-193, 1988.
8. C. Goradia, W. Thesling, M. Ghalla-Goradia, I. Weinberg and C.K. Swartz, "Predicted Performance of Near-optimally Designed Indium Phosphide Space Solar Cells at High Intensities and Temperatures", Conf. Rec. 20th IEEE Photovoltaic Specialists Conf., Sept. 26-30, 1988, Las Vegas, Nevada.

9. C. Goradia, W. Thesling, M. Ghalla-Goradia, I. Weinberg and C.K. Swartz, "Predicted Performance of InP Solar Cells in Cassegrainian and Slats Space Concentrator Arrays at 20 to 100 AMO, 80° to 100° C", Proc. Ninth Space Photovoltaic Research and Technology Conf., NASA Lewis Research Center, April 19-21, 1988, pp. 70-82.

10. C. Goradia, J.V. Geier and I. Weinberg, "Experimental and Theoretical Comparison of 1MeV Electron Induced Radiation Damage in InP and GaAs Space Solar Cells", Proc. Third International Photovoltaic Science and Engineering Conf., Nov. 3-6, 1987, Tokyo, Japan, pp. 207-210.

11. R. O. Clark, C. Goradia, and D. J. Brinker, "Dependence of Lifetime on Design Parameters of nipi Doping Superlattice: Results of Self-Consistent Calculations", Third International Conference on Superlattices, Microstructures and Microdevices, August 16-20, 1987, Chicago, Illinois, only abstract.

12. R.O. Clark, C. Goradia, D.J. Brinker, "Self-consistent Calculations and Design Considerations for a GaAs nipi Doping Superlattice Solar Cell", Conf. Rec. 19th IEEE Photovoltaic Specialists Conf., May 4-8, 1987, New Orleans, LA, IEEE Publ. No. 87CH2400-0, pp. 133-139.

13 J. Stupica, C. Goradia, C.K. Swartz and I. Weinberg, "Radiation Damage and Defect Behavior in Proton Irradiated Lithium-Counterdoped n+p Silicon Solar Cells", Conf. Rec. 19th IEEE Photovoltaic Specialists Conf., May 4-8, 1987, New Orleans, LA, IEEE Publ. No. 87CH2400-0, pp. 650-654.

14. C. Goradia, J.V. Geier and I. Weinberg, "Modelling and Design of High Efficiency, Radiation Tolerant Indium Phosphide Space Solar Cell", Conf. Rec. 19th IEEE Photovoltaic Specialists Conf. May 4-8, 1987, New Orleans, LA, IEEE Publ. No. 87CH2400-0, pp. 937-943.

15. Maria Faur, M. Faur, G. Goradia, D. Jayne, F. Honey and I. Weinberg, "XPS, Auger and SEM Analysis of the InP Surface After Closed-Ampoule Diffusion with Sulfur at Several Diffusion Temperatures", Proceedings of the 1st International Conf. on Indium Phosphide and Related Materials for Advanced Electronic and Optical Devices, Norman, USA, March 20-22, 1989, SPIE Vol. 1144, p 501, 1989.

16. M. Faur, Maria Faur, C. Goradia, M. Goradia, N. Fatemi, D. Brinker and R. Thomas : "Indium Phosphide Solar Cells Made by Closed-Ampoule Diffusion of Sulfur into Cd-doped InP Substrates: Dependence of Cell

Characteristics on Diffusion Temperature and Time", *ibid* SPIE Vol.1144, 489, 1989.

17. Maria Faur, M.Faur, C.Goradia, D.Jayne, N.Fatemi and D.Brinker : "XPS Investigation of the InP/Anodic Oxide Interface of the n+p InP Solar Cell Fabricated by Thermal Diffusion of Sulfur through an Anodic Oxide Cap", 11th Symposium on Applied Surface Analysis, Cleveland, OH, May 31-June 2, 1989.

18. M.Faur, Maria Faur, C.Goradia, D.Jayne, P.Jenkins, S.Bailey and I.Weinberg, "XPS Investigation of the Native Oxide on Sulfur Diffused n+InP Surface as a Function of Diffusion Time and Temperature for Surface Passivation of InP Solar Cells", *ibid*, 1989.

19. M.Faur, Maria Faur, C.Goradia, M.Goradia, R.D.Thomas, N.Fatemi and F.Honey, "A Comparative Study of Performance Parameters of n+p InP Solar Cells Made by Closed-Ampoule Sulfur Diffusion into Cd- and Zn-Doped p-type InP Substrates", Proceedings of the 10th Space Photovoltaic Research and Technology (SPRAT) Conference, Cleveland, OH, Nov.7-9, 1989, p.332.

20. Maria Faur, M.Faur, M.Goradia, P.Jenkins, D.Jayne and I.Weinberg, "Investigation of Anodic and Chemical Oxides Grown on p-type InP with Applications to Surface Passivation for n+p InP Solar Cell Fabrication", *ibid*, p 316.

21. Maria Faur, M.Faur, M.Goradia and S.Bailey, "Anodic Dissolution of InP", Proceedings of the 2nd International Conference on Indium Phosphide and Related Materials, Denver, CO, April 23-25, 1990, IEEE Catalog #90CH2859-7, p 242.

22. M.Faur, I.Weinberg, Maria Faur, C.Goradia and R.Clark, "Dislocation Density After S-Diffusion into p-type InP Substrates", *ibid*, p 397, 1990.

23. S.Bailey, N.Fatemi, G.A.Landis, D.Brinker, M.Faur and Maria Faur: "Application of V-Groove Technology to InP Solar Cells", *ibid*, p 73.

24. M.Faur, Maria Faur, P.Jenkins, M.Goradia, S.Bailey, D.Jayne, I.Weinberg and C.Goradia : "Study of Surface Passivation as a Function of InP Closed-Ampoule Solar Cell Fabrication Processing Variables", Proceedings of the 21st IEEE Photovoltaic Specialists Conference (PVSC), Kissimmee, USA, May 21-

25, 1990, Vol.1, p 130.

25. P.Jenkins, M.Goradia, M.Faur, S.Bailey and Maria Faur, "Measurement of Surface Recombination Velocity on Heavily Doped Indium Phosphide", *ibid*, Vol.1, p 399.

26. Maria Faur, M.Faur, D.T.Jayne, M.Goradia and C.Goradia : "XPS Investigation of Anodic Oxides Grown on p-type InP", *Surface and Interface Analysis*, 15, p 641, 1990.

27. M.Faur, Maria Faur, P.Jenkins, M.Goradia, S.Bailey, D.Jayne, I.Weinberg and C.Goradia : "Study of Surface Passivation of InP", *Surface and Interface Analysis*, 15, p745, 1990.

28. M.Faur, Maria Faur, F.Honey, C.Goradia, M.Goradia, R.Clark and D.Jayne, "Closed-Ampoule Diffusion of Sulfur into Cd-doped InP Substrates: Dependence of S Profiles on Temperature and Time", *J.of Vacuum Sci.and Technology*, B 10(4), p.1277, 1992.

29. M.Faur, Maria Faur, C.Goradia, M.Goradia and I.Weinberg, " High Quality Thermally Diffused  $p^+n$  InP Structures", *Proceedings of the 3rd International Conference on InP and Related Materials*, Cardiff, Wales, UK, April 8-11, 1991, p 304.

30. Maria Faur, M.Faur, C.Vargas and M.Goradia , "EC-V Profiling of InP", *ibid*, p 130.

31. M.Faur, Maria Faur, D.J.Flood, I. Weinberg, D.J.Brinker, C.Goradia, M.Goradia and W.Thesling : "A Comparative Study of  $p+n$  and  $n^+p$  InP Solar Cells Made by a Closed-Ampoule Diffusion", *Proceedings of the 11th Space Photovoltaic Research and Technology Conference*, Cleveland, OH, May 7-9, 1991, p 3-1.

32. Maria Faur, M.Faur, I.Weinberg, M.Goradia and C.Vargas : "High Resolution Electrolyte for Thinning InP by Anodic Dissolution and its Applications to EC-V Profiling, Defect Revealing and Surface Passivation", *ibid*, p.3-1.

33. M.Faur, Maria Faur, D.J.Flood, D.J.Brinker, I.Weinberg, C.Goradia and W.Thesling , "High Voltage Thermally Diffused  $p+n$  InP Solar Cells", *Proceedings of the 22nd IEEE Photovoltaic Specialists Conference*, Las

Vegas, Oct 7-11 ,1991, p.439.

34. Maria Faur, M.Faur, S.Bailey, D.J.Brinker, M.Goradia, I.Weinberg and N.Fatemi "High Performance Etchant for Thinning  $p+n$  InP and its Applications to  $p+n$  InP Solar Cell Fabrication", *ibid*, p.241.

35. I.Weinberg, P.Jenkins, Maria Faur, D.J.Brinker and H.B.Curtis, "Carrier Remover in Heavily Doped InP Structures", 22nd IEEE PVSC, p.1445, 1991.

36. I.Weinberg, C.K.Schwartz, H.B.Curtis, D.J.Brinker, P.Jenkins, and Maria Faur, "Effect of Dislocations on the Properties of Heteroepitaxial InP Solar Cells", 11th SPRAT Conf., p 6-1, 1991

37. M.Faur, Maria Faur, C.Goradia, M.Goradia and I.Weinberg, "Defect Density Reduction of  $n+p$  and  $p+n$  InP Structures Fabricated by Closed-Ampoule Thermal Diffusion", Proceedings of the 4th Int. Conf.on InP and Related Materials, Newport, Rhode Island, April 20-24, 1992, p.322.

38. Mircea Faur, Maria Faur, C.Goradia, M.Ghala, and I.Weinberg, "Low Processing Cost InP Solar Cells for Space Applications", 2nd Symposium on Aerospace Challenges in Northern Ohio, May 27, 1992.

39. Mircea Faur, Maria Faur, C.Goradia, M.Goradia, D.J.Flood, D.J.Brinker, I.Weinberg and N.S.Fatemi, "Progress in  $p+n$  InP Solar Cells Fabricated by Thermal Diffusion" Proceedings at the 12th Space Photovoltaic Research and Technology Conference, Oct.20-22, 1992, p.23.

40. Maria Faur, Mircea Faur, M.Goradia, C.Vargas-Aburto and D.M.Wilt, "Electrochemical Characterization of InP Structures", *Ibid*, p.33.

41. Mircea Faur, Maria Faur, D.J.Flood, D.J.Brinker, C.Goradia, M.Goradia, I.Weinberg and N.Fatemi, "Experiment-Based Projected High Efficiency InP Solar Cells for Space Applications", Proceedings of the 5th Int'l Conference on InP and Related Materials, Paris, France, April 21-24, 1993, p.218.

42. Maria Faur, Mircea Faur, M.Goradia, and C.Vargas, "Design of High Quality Thermally Diffused  $p+n$  and  $n+p$  InP Structures by Electrochemical Studies, *ibid*, p.615.

43. Mircea Faur, "Radiation Resistance of InP Solar Cells", PhD Dissertation Thesis, Bucharest University, Romania, February 1993, 265 pp.

44. Mircea Faur, Maria Faur, D.J.Flood, D.J.Brinker, I.Weinberg, C.Goradia and M.Goradia, "Low Carrier Removal Rates and Annealing Behavior of Thermally Diffused  $p^+n$ (Cd,S) InP Structures After  $10^{13}\text{cm}^{-2}$  3 MeV Proton Irradiation", Proceedings at the 23rd IEEE Photovoltaic Specialists Conference, KY, May 10-14, 1993, p.1437.

45. Maria Faur, Mircea Faur, S.Bailey, M.Goradia, G.Mateescu and V.Voljin, "High Resolution Etchants and Electrolytes for Accurate Revealing of Surface and Deep Precipitates of InP", *ibid*, p.747.

46. Maria Faur and Mircea Faur, "High Resolution Electrolyte for Thinning InP by Anodic Dissolution and its Application to EC-V Profiling, Defect Revealing and Surface Passivation, CSU Patent Pending, 1993.

47. Mircea Faur, Maria Faur, D.T.Jayne, S.Bailey and M.Goradia, "Chemical Thinning of InP Diffused Structures", 15th Symposium on Applied Surface Analysis, Cleveland, June 7-8, 1993.

48. Maria Faur, Mircea Faur, G.Mateescu, C.Goradia, and V.Voljin, "New Etchants and Electrolytes for Accurate Revealing of Structural Defect Densities of InP Substrates and Structures", *ibid*, 1993.

49. Mircea Faur, Maria Faur, D.T.Jayne, S.Bailey and M.Goradia, "Etchant for Chemical Thinning of InP and its Application in the Fabrication of InP Diffused Junction Solar Cells", *Surface and Interface Analysis*, 21, 110 (1994).

50. Maria Faur, Mircea Faur, D.J.Flood and M.Goradia, "Electrolyte for Electrochemical C-V Profiling of InP- and GaAs- Based Structures", *Materials Science and Engineering B28*, 31(1994).

51. Mircea Faur, Maria Faur, D.J.Flood, D.J.Brinker, C.Goradia, S.Bailey, I.Weinberg, M.Goradia, D.T.Jayne, J.Moulot and N.Fatemi, "Effective First Layer Antireflective Coating on InP Solar Cells Grown by Chemical Oxidation", Proceedings of the 6-th Int'l Conference on Indium Phosphide and Related Materials, Santa Barbara, California, March 28-31, 1994, p.492.



52. Maria Faur, Mircea Faur, D.J.Flood, M.Goradia and D.M.Wilt, "Electrolyte for EC-V Profiling of InP and GaAs Based Heterostructures", *ibid*, p.508.

53. Maria Faur, Mircea Faur, D.J.Flood and M.Goradia, "High Resolution Electrolyte for Electrochemical C-V Profiling of InP and GaAs Based Structures", 2-nd Int'l Workshop on Expert Evaluation and Control of Compound Semiconductor Materials and Technologies, Parma, Italy, May 18-20, 1994.

54. Mircea Faur, Maria Faur, D.J.Flood, P.Jenkins, D.J.Brinker, I.Weinberg and C.Goradia, "Low Defect Density  $p^+n(Cd,S)InP$  Diffused Structures", *ibid*, 1994.

55. Mircea Faur, Maria Faur, D.J.Flood, D.J.Brinker, C.Goradia, N.S.Fatemi, P.P.Jenkins, D.M.Wilt, S.Bailey, M.Goradia and J.Moulot, "Status of Diffused Junction  $p^+n$  InP Solar Cells for Space Applications", Proceedings of the XIII Space Photovoltaic Research and Technology Conference, June 14-16, 1994, pp. 63-79.

56. Mircea Faur, Maria Faur and David Epperley, "Ultra-High Purity Still Electric Still Water System," CSU patent pending, 1994.

57. Mircea Faur, Maria Faur, D.J.Flood, C.Goradia, D.J.Brinker, M.Goradia, N.Fatemi, P.P.Jenkins, S.Bailey, D.M.Wilt and J.Moulot, "Status of  $p/n$  Diffused Junction Solar Cells for Space Power Applications", to appear in Proceedings of the 1st World Conference on Photovoltaic Energy Conversion, Hawaii, Dec.5-9, 1994.

58. Maria Faur, Mircea Faur, D.J.Flood, P.P.Jenkins, M.Goradia and D.Wilt, "Electrochemical Characterization of InP and GaAs Based Structures for Space Solar Cell Applications, *ibid* 1994. 1994.

59. J.Moulot, Mircea Faur, Maria Faur, C. Goradia, M. Goradia and S. Bailey, "Three-Layer Antireflecting Coating for High Efficiency InP Solar Cells," 14th Space Photovoltaic Research and Technology Conference, Oct. 24-26, 1995.

## General References (GR)

- [1] H. Okazaki, T. Takamoto, H. Takamura, T. Kamei, M. Ura, A. Yamamoto and M. Yamaguchi, "Production of Indium Phosphide Solar Cells for Space Power Generation", Proceedings of the 20th IEEE Photovoltaic Specialists Conference, p. 886 (1988).
- [2] R. J. Walters and G.P. Summers, "A Detailed Study of Photo-Injection Annealing of InP Solar Cells", 11th Space Photovoltaics Research and Technology Conference, Cleveland, OH, Oct. 20-22 (1992).
- [3] S. R. Messenger, R. J. Walters, and G. P. Summers, "High Temperature Annealing of Minority Carrier Traps in Irradiated MOCVD  $n^+p$  InP Solar Cell Junctions", Ibid., (1992).
- [4] C. J. Keavney, V. E. Haven and S. M. Vernon, "Emitter Structures in MOCVD InP Solar Cells", Proceedings of the 2nd International Conference on InP and Related Materials, IEEE Catalog #90CH2859-7, p. 435 (1990).
- [5] Itoh, M. Yamaguchi and C. Uemura, "17.2% Efficient (AM0)  $p^+-i-n$  InP Homojunction Solar Cells", IEEE Electron Device Letters, EDL-7 (2), 127 (1986).
- [6] K. Y. Choi, C. C. Shen, and B. I. Miller, "p/n Homojunction Solar Cells by LPE and MOCVD Techniques".

Table 1. Measured or Projected AMO, 25°C n/p and p/n InP Solar Cell Performances.

Structure	Junction formation technique	Dopant	Approx Junction depth ( $\mu\text{m}$ )	$V_{oc}$ (mV)	$J_{sc}$ (mA/cm <sup>2</sup> )	FF (%)	$\eta$ (%)	Ref.
n <sup>+</sup> (InGaAs) / n(InP) / p(InP) / p <sup>+</sup> (InP)	MOCVD	Si/Zn	0.025	876	36.34	82.4	19.1	GR.[4]
n <sup>+</sup> -p	Closed Ampoule	S/Zn	0.2-0.3	828	33.7	81.6	16.6	GR.[1]
n <sup>+</sup> -p	Closed Ampoule	S/Cd	0.15 0.08-0.1	806 840	30.5 36.5	80.1 84	14.35 <sup>(a)</sup> 18.8 <sup>(b)</sup>	R.[16]
p <sup>+</sup> -i-n	LPE	Mg/S	0.6	823.7	37.6 (active area)	75.4	17.2	GR.[5]
p <sup>+</sup> (InGaAs) / p <sup>+</sup> (InP) / n(InP) n <sup>+</sup> (InP)	LPE MOCVD	Zn/S	0.7	866 864	29.25 32.84	81 76.7	15 15.9	GR.[6]
p <sup>+</sup> -n	Closed Ampoule	Cd/S	0.25 0.62 0.3 0.25	860 880.3 895 910	29.1 26.8 37.5 38.2	52.2 73.1 82 84	9.52 12.57 <sup>(c)</sup> 20.1 <sup>(d)</sup> 21.3 <sup>(e)</sup>	R.[55] R.[55]

(a) Measured on cells with unoptimized AR coating, and front contacts; (b) experimental-based projected maximum practically achievable performances; (c) Measured values on bare cell,  $R_s \sim 3\Omega \text{ cm}^{-2}$ , front grid coverage: 10.55%; (d) Projected parameters of cell above by using an optimized AR coating, reducing the grid shadowing to 6% and reducing  $R_s$  to  $\sim 0.5\Omega \text{ cm}^{-2}$ ; and (e) Maximum practically achievable projected parameters using our state-of-the-art diffused structures with a net surface acceptor concentration of  $4 \times 10^{18} \text{ cm}^{-3}$ .

Table 2: AM0, 25°C performances of selected p<sup>+</sup>n (Cd,S) InP diffused junction solar cells

Cell #	AR Coating	Approx. Emitter Thickness (μm)	Rs (Ω-cm <sup>2</sup> )	Jsc (mA/cm <sup>2</sup> )	Voc (mV)	FF (%)	η (%)	Measured at
80 <sup>(a)</sup>	In <sub>2</sub> O <sub>3</sub> <sup>(c)</sup> (~1800 Å)/ In(PO <sub>3</sub> ) <sub>3</sub> <sup>(d)</sup> (~450Å)	0.5	3.3	26.64	884	73.7	12.65	SPIRE
83 <sup>(a)</sup>	In <sub>2</sub> O <sub>3</sub> <sup>(c)</sup> (~1500 Å)/ In(PO <sub>3</sub> ) <sub>3</sub> <sup>(d)</sup> (~400Å)	0.45 <sup>(e)</sup>	3.52	26.3	887.6	69	11.98	NASA
81 <sup>(a)</sup>	In <sub>2</sub> O <sub>3</sub> <sup>(c)</sup> (~1500 Å)/ In(PO <sub>3</sub> ) <sub>3</sub> <sup>(d)</sup> (~400Å)	0.45	3.65	27.18	888	69.2	12.17	SPIRE
89 <sup>(b)</sup>	In(PO <sub>3</sub> ) <sub>3</sub> <sup>(d)</sup> (~400Å)	0.45 <sup>(e)</sup>	3.24	27.5	884.6	73.7	12.95	NASA
91 <sup>(b)</sup>	In <sub>2</sub> O <sub>3</sub> <sup>(c)</sup> (~900 Å)/ In(PO <sub>3</sub> ) <sub>3</sub> <sup>(d)</sup> (~300Å)	0.4	3.35	28.2	881.7	72.6	13.2	NASA
84 <sup>(b)</sup>	In <sub>2</sub> O <sub>3</sub> <sup>(c)</sup> (~1500 Å)/ In(PO <sub>3</sub> ) <sub>3</sub> <sup>(d)</sup> (~400Å)	0.35	3.75	28.31	883	67.9	12.37	SPIRE
85 <sup>(a)</sup>	In(PO <sub>3</sub> ) <sub>3</sub> (~300Å)	0.30 <sup>(e)</sup>	4.92	27.6	886.9	62.8	11.25	NASA
87 <sup>(a)</sup>	In <sub>2</sub> O <sub>3</sub> (~1100 Å)/ In(PO <sub>3</sub> ) <sub>3</sub> (~400Å)	0.3	4.38	29.4	877.2	61.7	11.63	NASA
	In(PO <sub>3</sub> ) <sub>3</sub> (~400Å)			27.6	886.6	62.8	11.25	
	SiO (~850Å)/ In(PO <sub>3</sub> ) <sub>3</sub> (~400Å)			30.95	887.5	61.5	12.36	

Cell area: 0.48 cm<sup>2</sup> ; front grid coverage: 9.55%; distance between fingers: 620 μm; front contact thickness: ~0.3μm

Diffusion conditions: 660 °C, 20 mins; Diffusion cap: In(PO<sub>3</sub>)<sub>3</sub>, thickness: (a) ~3nm, (b) ~10 nm; Surface acceptors concentration: ~3\*10<sup>18</sup> cm<sup>-3</sup>; Junction depth: (a) ~4.5 μm (graded profile near junction), (b) ~3.5 μm (near step profile). The residual chemical oxide after dissolving the p<sup>+</sup> InP emitter has two components: a thick In<sub>2</sub>O<sub>3</sub>-rich surface layer (c), and an interfacial In(PO<sub>3</sub>)<sub>3</sub>-rich layer (d). (e) measured values

Table 3: AM0, 25 °C experiment-based practically achievable predicted performances of cell #89

Emitter Thickness ( $\mu\text{m}$ )	AR Coating	Front Contact Pattern	Jsc ( $\text{mA}/\text{cm}^2$ )	Voc (mV)	FF (%)	$\eta$ (%)
0.45	In(PO <sub>3</sub> ) <sub>3</sub> (~400Å)	Grid coverage: 9.55 % Grid thickness: 0.3 $\mu\text{m}$ Distance between fingers: 620 $\mu\text{m}$	27.5	884.6	73.7	12.95
	Optimized In(PO <sub>3</sub> ) <sub>3</sub> (400Å)/ Al <sub>2</sub> O <sub>3</sub> (434Å)/ MgF <sub>2</sub> (602Å)		36.3	894	73.9	17.3
		SPIRE's mask: Grid coverage: 5.33 % Distance between fingers: 250 $\mu\text{m}$ Grid thickness: ~ 5 $\mu\text{m}$ .	38.0	896	84	20.6
0.2-0.3			38.6	910	84	21.3

**Table 4: AM1.5, 25°C performance parameters of a diffused p<sup>+</sup>n (Cd,S) InP solar cell before (b) and after irradiation with 10<sup>13</sup> cm<sup>-2</sup>, 3MeV protons.**

Time after irradiation (hours)	Voc (mV)	Jsc (mA/cm <sup>2</sup> )	FF (%)	(%)	Rs (-cm <sup>2</sup> )
0 (b)	871	27.42	72.64	12.65	3.27
8	664	15.48	64.00	4.86	5.33
90	676	16.37	65.10	5.25	5.19
206	682	16.85	65.50	5.49	4.88
857	708	18.47	66.00	6.29	4.85

The cell was kept at RT in the dark except for 6 short exposures to light during illuminated I-V measurements

**Table 5: AM0, 25°C performance parameters of a p<sup>+</sup>n (Cd,S) InP solar cell (same as in Table 2), before (b) irradiation and (a) 1 year after irradiation with 10<sup>13</sup> cm<sup>-2</sup> 3MeV protons.**

	Voc (mV)	Jsc (mA/cm <sup>2</sup> )	FF (%)	$\eta$ (%)
(b)	880.3	26.81	73.1	12.57
(a)	713.9	18.02	67.0	6.31

Measurements performed at NASA LeRC. After irradiation, the cell was kept at RT in the dark except for 6 light exposures during the AM1.5, 25°C illuminated I-V measurements in Table 2.

**Table 6. AM0, 25 °C performance parameters of a CSU p<sup>+</sup>n InP solar cell prior to and after -irradiation at 1 MeV equivalent electron fluence of 1.06x10<sup>17</sup> cm<sup>-2</sup>.**

	Voc (mV)	Jsc (mA/cm <sup>2</sup> )	FF (%)	$\eta$ (%)	Jo <sub>1</sub> (n <sub>1</sub> =1) (A/cm <sup>2</sup> )	Jo <sub>2</sub> (n <sub>2</sub> =2) (A/cm <sup>2</sup> )	R <sub>s</sub> ( $\Omega$ -cm <sup>2</sup> )
Before irradiation	888	27.18	69.21	12.17	2.8*10 <sup>-17</sup>	7.7*10 <sup>-11</sup>	3.66
Post irradiation	652	13.64	60.14	3.90	2.7*10 <sup>-14</sup>	3.4*10 <sup>-8</sup>	6.04
After 4 days at RT in the dark	659	14.32	60.14	4.13	2.1*10 <sup>-14</sup>	3.05*10 <sup>-8</sup>	5.91

The measurements and irradiation were performed at SPIRE Corp. , and presented here with permission from Dr. C. Blatchley .



**Table 7. Surface EPD and precipitates of  $n^+p$  InP structures diffused at 660°C through bare and capped surfaces**

Structure	Diffusion Cap	Surface EPD ( $\text{cm}^{-2}$ )	Surface Precipitates	Deep
$n^+p$ (S,Zn)	Bare	$6 \times 10^8$	$\text{In}_2\text{S}_3$	ZnS
$n^+p$ (S,Cd)	Surface	$3 \times 10^7$	$\text{In}_2\text{S}_3$	--
$n^+p$ (S,Zn)	$\text{In}(\text{PO}_3)_3$	$8 \times 10^6$	$\text{In}_2\text{S}_3$	--
$n^+p$ (S,Cd)	(~ 5 nm)	$6 \times 10^5$	$\text{In}_2\text{S}_3$	--

**Table 8. Surface EPD and precipitates in  $p^+n$  InP structures.**

Structure	Diffusion Cap	Diffusion Temp ( $^{\circ}\text{C}$ )	Surface EPD ( $\text{cm}^{-2}$ )	Surface Precipitates	Deep
$p^+n$ (Zn,S)	Bare	520	$5 \times 10^7$	$\text{Zn}_3\text{P}_2$	$\text{Zn}_3\text{P}_2$
$p^+n$ (Cd,S)	Surface	560	$7 \times 10^5$	$\text{Cd}_3\text{P}_2$	--
$p^+n$ (Zn,S)	$\text{In}(\text{PO}_3)_3$	520	$3 \times 10^5$	$\text{Zn}_3\text{P}_2$	$\text{Zn}_3\text{P}_2$
$p^+n$ (Cd,S)	(~ 4 nm)	560	$2 \times 10^2$	--	--

Table 9. EC-V PROFILING OF InP and GaAs BASED STRUCTURES

Recommended electrolytes for EC-V profiling of selected III-V compound semiconductors

Electrolyte/ Material	HCl	Tiron	Pear etch	EDTA	AT	FAP
InP	x		x			x
GaAs		x		x	x	
InGaAs	x			x	x	
InGaP	x					
GaAsP		x				
AlGaAs		x		x	x	
InGaAsP	x				x	

HCl = 0.5 M HCl in water [2];

Tiron = 1,2-dihydroxybenzene-3,5-disulfonic acid disodium salt,  $C_6H_2(OH)_2(SO_3Na)_2 \cdot H_2O$  [3];

pear etch = 37% HCl-70%  $HNO_3$ -methanol (36:24:1000) [4];

EDTA = 0.1 M  $Na_2EDTA$  basified with ethylenediamine to pH 9.1 [5];

ammonium tartrate (AT) =  $(NH_4)_2C_4O_6$ , basified with aqueous  $NH_3$  to pH 11.5 or higher [5];

FAP = 48% HF-99%  $CH_3COOH$ -30%  $H_2O_2$ - $H_2O$ (10:2:1:200) [6].

#### References

- [1] T. Ambridge and M.M. Faktor, *J. Appl. Electrochem.*, 5, 319 (1975).
- [2] T. Ambridge and D.J. Ashen, *Electron Lett.* 15, 674 (1979).
- [3] M.M. Faktor and J.L. Stevenson, *J. Electrochem. Soc.*, 125, 621 (1978).
- [4] R.T. Green, D.K. Walker and C.M. Wolfe, *J. Electrochem. Soc.*, 133(11), 2278 (1986).
- [5] PN 4200 Polaron Semiconductor Profiler, BIORAD, Instruction Manual (1988).
- [6] M.Faur, M. Faur, C.Vargas and M. Goradia, Proc.2nd IPRM Conf. UK, April 8-11, 1991, p. 130.

### Three-layer AR Coating Design with $\text{In}(\text{PO}_3)_3$ oxide as first layer

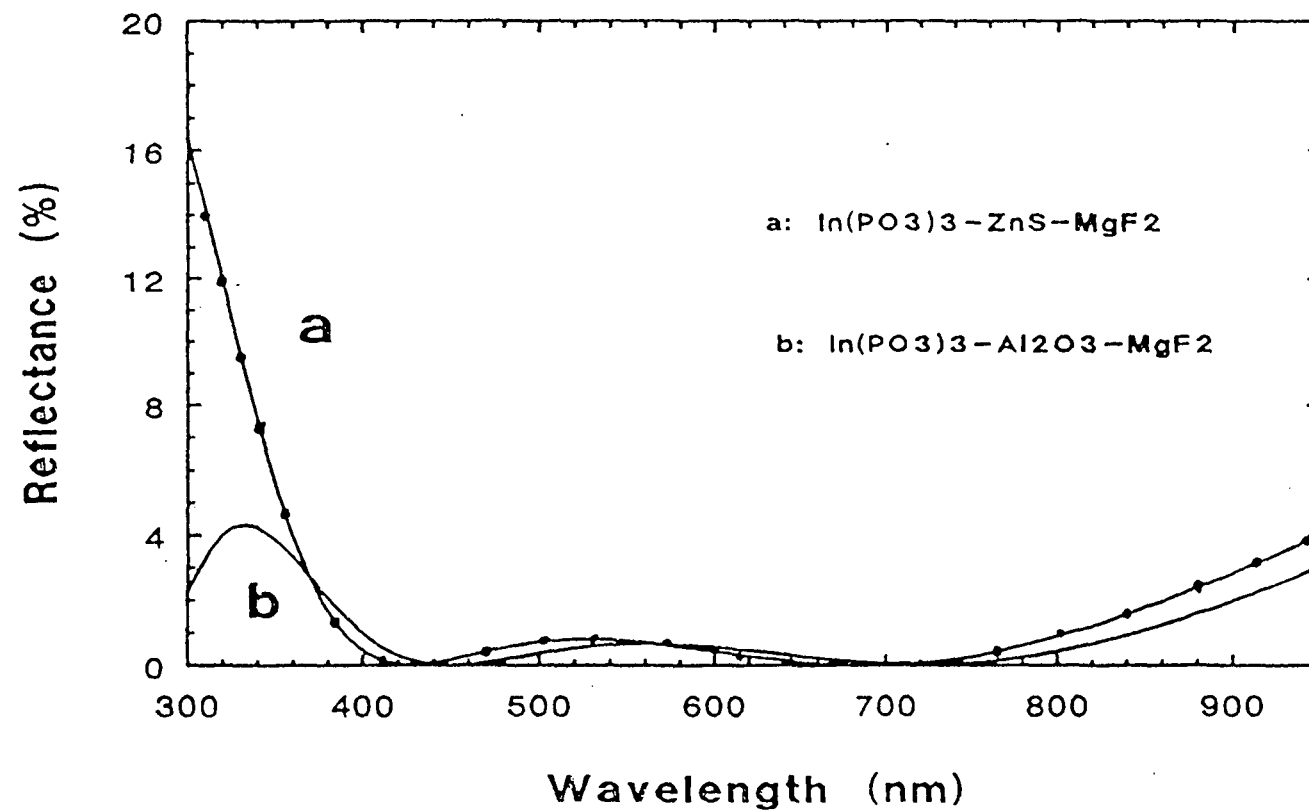


Fig. 1. Reflectance on optimized Three-layer AR coating using: a)  $\text{In}(\text{PO}_3)_3/\text{ZnS}/\text{MgF}_2$  b)  $\text{In}(\text{PO}_3)_3/\text{Al}_2\text{O}_3/\text{MgF}_2$

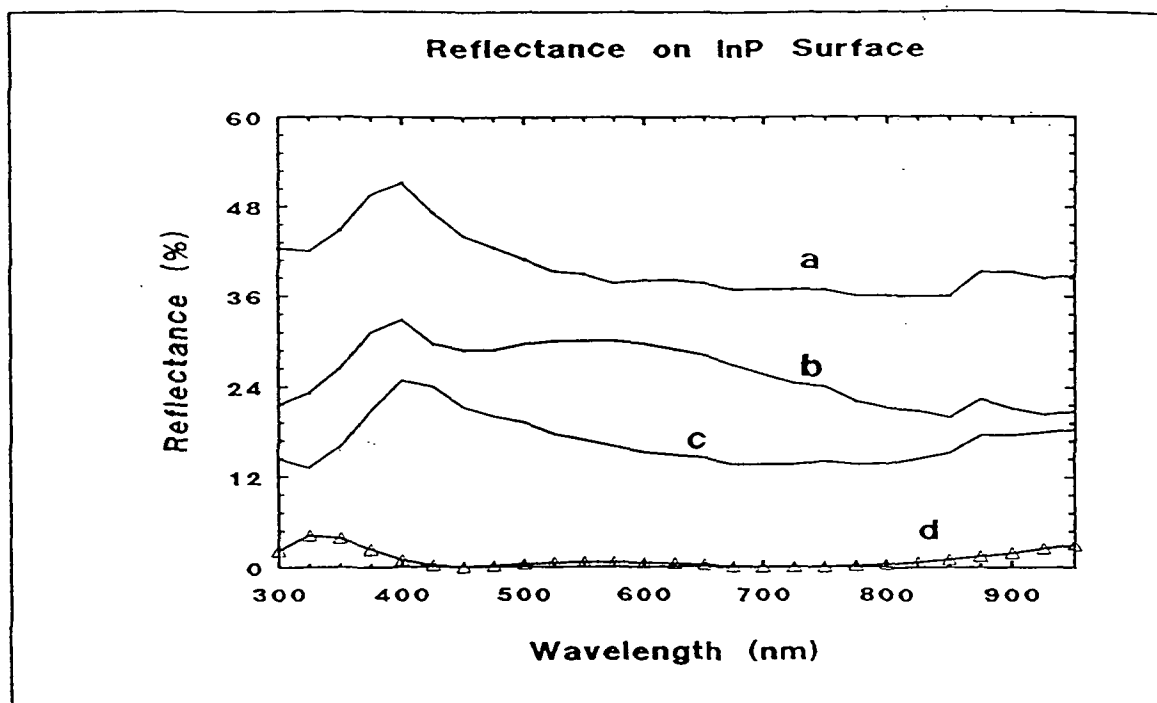


Fig. 2: Surface reflectance vs. wavelength of a) a bare  $p^+n$  InP surface (no oxide), no grid fingers;  $p^+n$  InP solar cells with: b) 10.5% grid coverage, 400 Å thick surface oxide layer; c) 10.5% grid coverage and 750 Å surface oxide; d) a 3-layer AR coating,  $\text{In}(\text{PO}_3)_3/\text{Al}_2\text{O}_3/\text{MgF}_2$ .

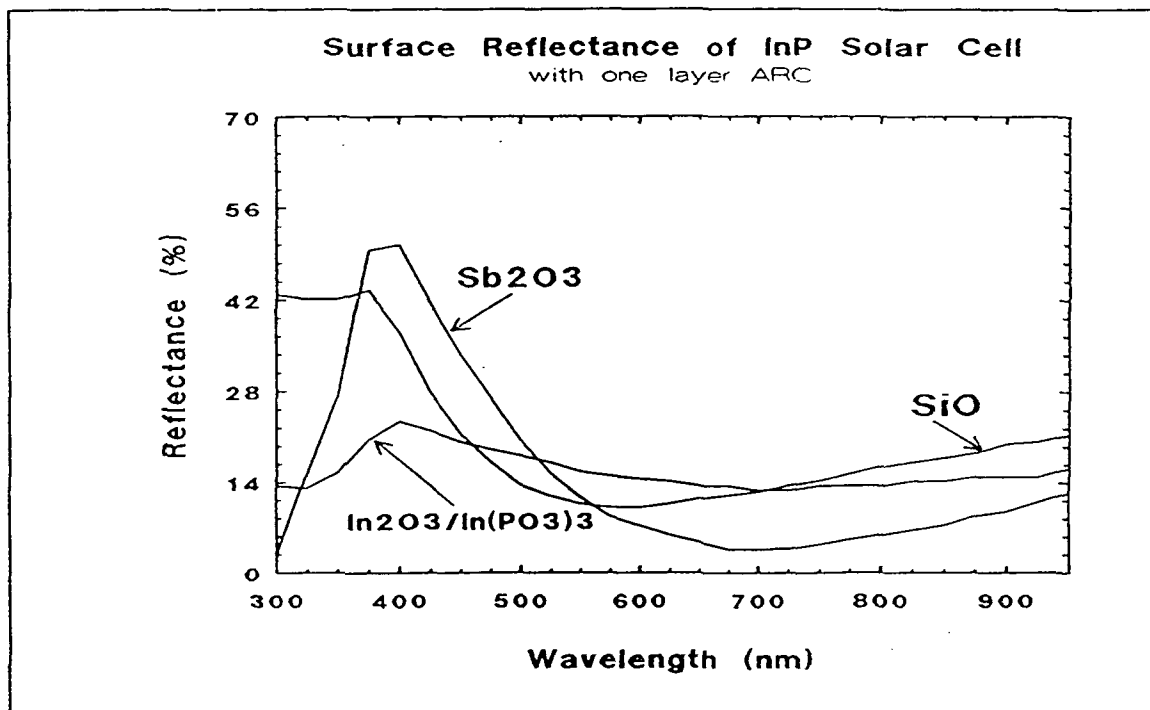


Fig. 3: Surface reflectance vs. wavelength of  $p^+n$  InP solar cells using single layer AR coating of the passivating chemical oxide ( $\text{In}_2\text{O}_3/\text{In}(\text{PO}_3)_3 \sim 1100/400\text{\AA}$ );  $\text{SiO}$  (800Å); and  $\text{Sb}_2\text{O}_3$  (750Å).